# Luminescence quantum efficiency and local optical density of states in thin film ruby made by ion implantation

T. M. Hensen, M. J. A. de Dood,[a] and A. Polman
*FOM Institute for Atomic and Molecular Physics, Kruislaan 407, 1098 SJ Amsterdam, The Netherlands*

(Received 19 June 2000; accepted for publication 4 August 2000)

Single crystal (0001) oriented, sapphire samples were implanted with 150 keV Cr ions at fluences between $6.0\times10^{14}$ and $4.0\times10^{15}$ Cr/cm$^2$. The peak concentrations ranged from 0.04 to 0.28 at %. Characteristic photoluminescence of the *R* lines at 694.3 and 692.9 nm was observed. Annealing at 1450 °C for 2 h increased the luminescence intensity by a factor of 45, due to the increasing fraction of substitutional Cr ions as confirmed by Rutherford backscattering spectrometry. The Cr luminescence decay rate in an annealed sample implanted with $3.0\times10^{15}$ at/cm$^2$ at 300 K is 299 s$^{-1}$. Decay rates were also measured for samples covered with a range of transparent liquids (refractive index $n=1.33-1.57$), showing a clear increase with increasing refractive index of the liquid. This effect is explained by the increase of the local optical density of states in the Cr-implanted region. By comparing the measured data with the calculated optical density of states the radiative decay rate is found to be $164\pm10$ s$^{-1}$ and the internal quantum efficiency ~50%. The quantum efficiency decreases slightly for increasing Cr concentration. © *2000 American Institute of Physics.* [S0021-8979(00)06021-7]

## I. INTRODUCTION

The spontaneous emission rate of an atom can be influenced by placing it close to a dielectric interface, within the scale of the emission wavelength, as first noted by Purcell.[1] Several experiments that demonstrate this concept have been performed and involve rare-earth ions or dyes in solution in contact with a dielectric or a mirror,[2–5] erbium ions implanted near a glass surface,[6] and electron-hole pairs recombining in a slab bound by two dielectrics.[7]

A theoretical description of the change in emission rate requires the quantization of the electromagnetic field and results in an expression of the decay rate in terms of a local density of states (DOS) of the (classical) Helmholtz equations.[8,9] In spatially inhomogeneous geometries the DOS changes from its free ($\epsilon=1$) value. For the case of a dielectric interface it can be calculated using Fermi's golden rule.[6,10–13]

While the simple case of a dielectric interface has now been well studied and understood, it appears challenging to study the modification of spontaneous emission in more complicated cases, involving, e.g., absorbing layers, strongly scattering systems, or photonic crystals. In order to do this, well-defined probes to measure the change in spontaneous emission rate are required. In this article we study the fabrication of thin film ruby ($Al_2O_3$:$Cr^{3+}$) layers that can be used as probes in such experiments.

The optical properties of transition metal ion solids have been studied for many years. Because the optical transitions of these ions occur in the outer lying 3*d* electronic levels of the ion, a strong coupling between these levels and the local crystal field of the surrounding atoms in the solid exists. If $Cr^{3+}$ ions are incorporated into $\alpha$-$Al_2O_3$ as substitutional atoms on the Al sublattice (known as ruby), characteristic *R* line luminescence is observed at well defined wavelengths of 692.9 and 694.3 nm. The energy levels are well understood in terms of ligand-field theory[14–16] and the luminescence was studied intensively since the introduction of the ruby laser.[17,18] Apart from its use as a laser, ruby can be used as a high-pressure or stress sensor. Here the pressure-induced frequency shift of the *R* lines, caused by a change in the local crystal field, is used for pressure or stress determination.[19–22]

Ion implantation is a relatively simple technique used to introduce Cr ions into the near-surface region of $Al_2O_3$. In the past much work has been done on the implantation of Cr ions to study surface hardening of $Al_2O_3$.[23–25] However these ion-implanted samples were never characterized by luminescence measurements. Luminescence of Cr ions close to a dielectric interface was studied in thin film ruby layers, formed by epitaxial growth, that were used as stress sensors.[26,27] In this case no attention was paid to luminescent lifetimes.

In this article we study $Al_2O_3$ implanted with $Cr^{3+}$ ions in the near-surface region, resulting in characteristic photoluminescence around 694 nm.[16] Subsequently the spontaneous emission is influenced by bringing liquid films with different refractive indices into contact with the surface of the Cr-doped $Al_2O_3$. The aim of this article is to determine the radiative lifetime and quantum efficiency of the *R* line luminescence for ion-implanted samples. Once characterized these samples can be used as probes of the local DOS in more complicated photonic systems.

## II. EXPERIMENT

One mm thick (0001) oriented $\alpha$-$Al_2O_3$ single crystals with low Cr content (<1 ppb) were implanted at room temperature with 150 keV $Cr^+$ ions to fluences of 0.6, 1.6, 2.5,

[a]Corresponding author; electronic mail: dood@amolf.nl

 

3.0, and $4.0\times10^{15}$ at/cm$^2$. The samples were rotated 7° with respect to the incoming Cr ion beam to avoid channeling in the [0001] crystal direction. The current on the sample during implantation was kept below 0.1 $\mu$A/cm$^2$. After implantation, the samples were annealed for 2 h at 1450 °C in air. One set of samples, implanted with $3.0\times10^{15}$ Cr/cm$^2$, was first annealed at 1200 °C for 1 h, and then at 1450 °C for 1 h.

Rutherford backscattering spectrometry (RBS) in combination with ion channeling was used to study the crystal structure before and after annealing, as well as the Cr depth distributions. A 2.0 MeV $^4He^+$ beam was used at a scattering angle of 165°. Photoluminescence (PL) measurements were performed at room temperature using the 457.9 nm line of an Ar-ion laser as a pump source. Typical pump powers of 15 mW in a 0.3 mm diam spot were used. The luminescence signal was detected using a 96 cm monochromator and a thermoelectrically cooled GaAs photomultiplier tube. The spectral resolution was 3.3 cm$^{-1}$. The pump beam was chopped at 13 Hz using an acousto-optic modulator and the signal was collected using standard lock-in techniques. Luminescence decay traces were recorded, at a spectral resolution of 8.3 cm$^{-1}$, using the GaAs photomultiplier tube in combination with a multichannel photon counting system. The overall time resolution was 400 ns.

Various liquids with different refractive indices were brought in contact with the implanted front side of the samples by inserting a droplet of the liquid between the sample and a fused silica slide, placed at a distance of ~1 mm from the sample. The Cr ions were pumped through the back side of the $Al_2O_3$ sample and the PL signal was collected from the back as well. The transparent liquids used are water ($n=1.33$), a mixture of ethylene glycol and water ($n=1.45$), microscope immersion oil ($n=1.51$), and 2-methoxy-4-propenylphenol ($n=1.57$).

## III. RESULTS AND DISCUSSION

Figure 1 shows RBS channeling measurements along the [0001] direction of $Al_2O_3$ samples implanted with $3.0\times10^{15}$ Cr/cm$^2$ before and after annealing. The dashed line shows a channeling spectrum of the as-implanted sample. A random spectrum (closed circles) is shown for reference. The dotted line shows the channeling spectrum after annealing at 1200 °C for 1 h. Annealing at 1450 °C for 1 h resulted in a spectrum (solid line) similar to that of a virgin sample (not shown). To show the implanted Cr distribution, the yield of the random and channeling spectra for the sample annealed at 1450 °C was multiplied by a factor of 50 for energies above 1.22 MeV.

Comparing the channeling spectrum of the as-implanted sample with the random spectrum shows that the implantation has caused a disordered region, but has not completely amorphized the $Al_2O_3$. The depth of maximum damage in the Al sublattice is around 100 nm, while the near-surface region is relatively damage free. Although clear channeling is observed in the Al sublattice, no channeling is observed in the O sublattice. This implies that the O sublattice, contrary to the Al sublattice, has been amorphized by the ion implantation. This difference between the Al and O sublattices was

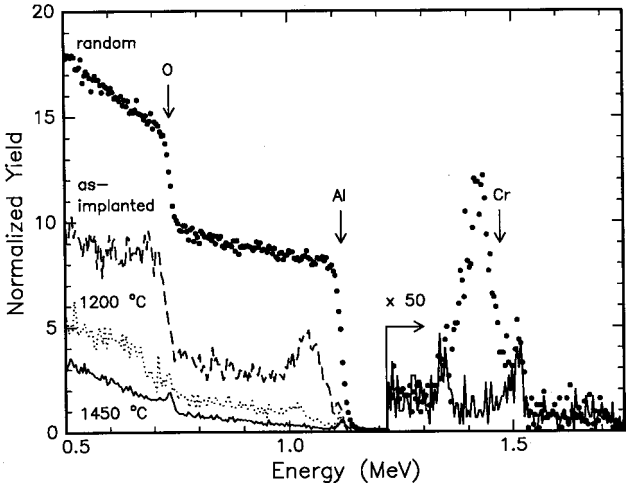


FIG. 1. RBS spectra of Cr-implanted ($3.0\times10^{15}$ Cr/cm$^2$) $Al_2O_3$. Channeling spectra are shown for the as-implanted sample and for samples annealed at 1200 and 1450 °C. A random spectrum after 1450 °C annealing is also shown. The Cr section in the spectrum is enlarged by a factor of 50 and is only shown for the random and channeled spectrum of the sample annealed at 1450 °C.

observed before in the annealing behavior of ion implanted $Al_2O_3$.[23–25] Figure 1 shows that annealing at 1200 °C for 1 h partly removes the damage made by the implantation (in both the Al and O sublattices). The damage is completely removed after subsequent annealing at 1450 °C for 1 h.

The random spectrum in Fig. 1 shows a Gaussian-shaped implanted Cr distribution, peaking at a depth of 70 nm and with a full width at half-maximum (FWHM) of 115 nm. Using this distribution and a density of $1.17\times10^{23}$ at./cm$^3$ for $Al_2O_3$ the implanted doses of 0.6, 1.6, 2.5, 3.0, and $4.0\times10^{15}$ Cr/cm$^2$ correspond to peak concentrations of 0.04, 0.11, 0.18, 0.21, and 0.28 at. % respectively. Note that diffusion of Cr in $Al_2O_3$ can be neglected for temperatures up to 1600 °C.[23,24] The small peak to the right of the surface energy of Cr is possibly due to a small amount of Fe (surface energy 1.51 MeV) either at the surface or co-implanted with the Cr. A comparison between the random and channeling RBS spectra for the Cr section in Fig. 1 shows that after annealing at 1450 °C the minimum yield of the Cr ions almost vanishes, indicating that the Cr ions are substitutional. The peak observed in the channeling spectrum around 1.33 MeV is most likely due to Cr ions that are not substitutional after annealing due to end-of-range damage caused by the Cr implantation. Our results indicate that at least 95% of the Cr ions are substitutional, in agreement with existing literature.[23,24] To summarize the RBS results, the first two columns of Table I list the minimum yield of the Al sublattice and the integrated minimum yield of the Cr distribution for the as-implanted sample and the samples annealed at 1200 and 1450 °C.

Figure 2 shows PL spectra measured at room temperature of $Al_2O_3$ samples implanted with $3.0\times10^{15}$ Cr/cm$^2$, after implantation and after annealing at 1200 and 1450 °C. All spectra show two distinct peaks at energies of 14 403 and 14 432 cm$^{-1}$ (corresponding to wavelengths of 694.3 and 692.9 nm, respectively), often identified as the $R_1$ and $R_2$

TABLE I. Minimum yield from RBS channeling measurements for the Al sublattice ($\chi^{Al}$) and the minimum yield integrated over the Cr depth distribution ($\chi^{Cr}$), measured after different anneal treatments. The normalized PL intensities and lifetimes measured at 694.3 nm ($R_1$ line) are also shown.

| | $\chi^{Al}$ (%) | $\chi^{Cr}$ (%) | $I_{PL}(R_1)$ | $W_{PL}$ ($s^{-1}$) |
|---|---|---|---|---|
| As implanted | 53 | 50 | 0.02 | 495 |
| 1200 °C | 13 | 70 | 0.26 | 361 |
| 1450 °C | 4 | 3 | 1.00 | 303 |

lines, respectively. The lines can be very well fitted with a sum of two Lorentzian line shapes.[28] For the sample that was annealed at 1200 °C, the FWHM of the 14 403 $cm^{-1}$ peak ($R_1$ line) is 15.2 $cm^{-1}$ and the FWHM of the 14 432 $cm^{-1}$ peak ($R_2$ line) is 11.4 $cm^{-1}$. After annealing at 1450 °C, the FWHM reduces to 12.7 and 9.72 $cm^{-1}$ (corresponding to 0.61 and 0.47 nm).

The $R_1$ and $R_2$ lines at 694.3 and 692.9 nm are characteristic for $Cr^{3+}$ ions that are substitutional on the Al sublattice.[16] The 457.9 nm line of the pump source is absorbed in the $^4T_1$ and $^4T_2$ broad bands.[29] Subsequently, rapid nonradiative relaxation to the first excited ($^2E$) state occurs, followed by radiative transition to the ground state ($^4A_2$).[17,18,29] The broadening of the $R$ lines is caused by Cr-lattice interaction. The FWHM measured in Fig. 2 is somewhat larger than that measured for bulk $Al_2O_3$:Cr. A possible explanation for this could be that the $Al_2O_3$ lattice contains residual damage or stress from the ion implantation that was not annealed completely[24] (but is invisible in RBS).

From Fig. 2 it is clear that the PL intensity increases with increasing anneal temperature. Although hard to identify in Fig. 2, the as-implanted sample shows two clear $R$ lines superimposed on a broad background. This is consistent

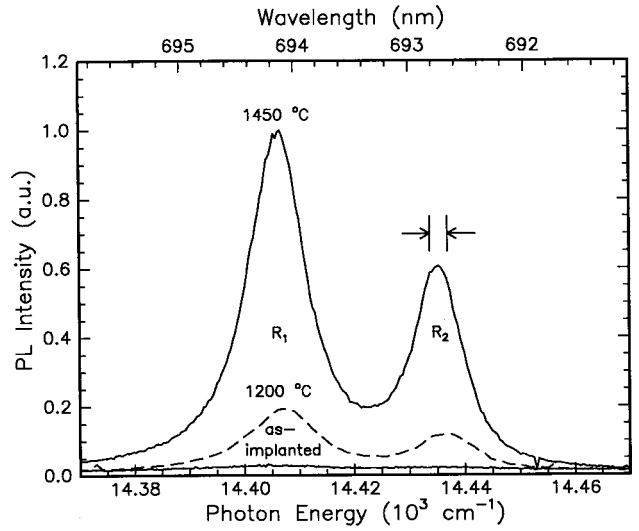


FIG. 2. Room temperature PL spectra of $Al_2O_3$ implanted with $3.0\times10^{15}$ Cr/cm$^2$ for various anneal treatments. Data are shown for the as-implanted sample, after annealing for 1 h at 1200 °C and after an additional anneal for 1 h at 1450 °C. Clear $R$ line luminescence is observed peaking at 14 403 (694.3 nm) and 14 432 $cm^{-1}$ (692.9 nm). The spectral resolution is indicated by the arrows. The pump wavelength is 457.9 nm and the pump power is 15 mW in a 0.3 mm diam spot.

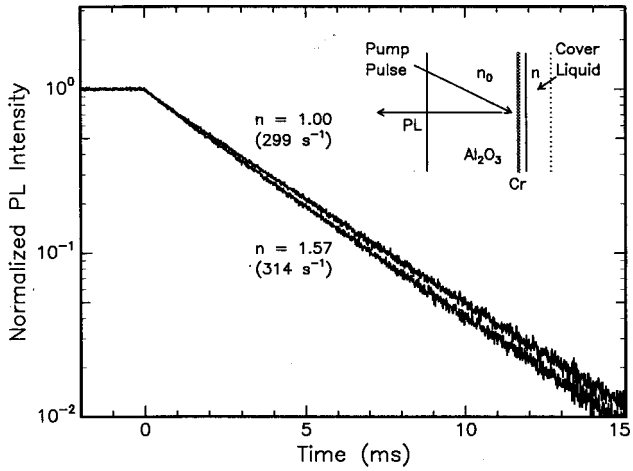


FIG. 3. Decay traces ($\lambda=694.3$ nm) for an $Al_2O_3$ sample implanted with $3.0\times10^{15}$ Cr/cm$^2$ (annealed 2 h at 1450 °C) measured in air and when in contact with 2-methoxy-4-propenylphenol ($n=1.57$). The PL was collected from the back of the sample as shown in the inset. The curve measured in air ($n=1.00$) shows a decay rate of 299 $s^{-1}$. An increase in the decay rate to 314 $s^{-1}$ is observed if the sample is covered with the liquid. The 457.9 nm pump light is switched of at $t=0$.

with channeling measurements[24] that show evidence of a small substitutional Cr fraction after implantation. Annealing at 1200 °C enhances the intensity by a factor of 12; subsequent annealing at 1450 °C yields a factor of 45 higher intensity than that of the as-implanted sample. An increase in intensity may be explained by an increase in concentration of substitutional Cr as well as by an increase in luminescence quantum efficiency. Luminescence lifetime measurements were performed at 694.3 nm to study the latter. The measured decay rates are 495, 361, and 303 $s^{-1}$ for the as-implanted and 1200 and 1450 °C annealed samples, respectively. The decay rates are listed in Table I together with the peak luminescence intensity of the $R_1$ line at 14 402 $cm^{-1}$. The measured decrease in decay rate of only a factor of 1.6 upon annealing implies that the 45-fold increase in PL intensity is mainly due to an increase in the concentration of substitutional Cr after annealing.

Due to additional nonradiative processes the measured decay rate will be higher than the radiative decay rate. It is known that ion implantation introduces defects and lattice strain in the crystal[24] which may not be completely removed by thermal annealing, leading to line broadening like in Fig. 2 and nonradiative decay channels. The total decay rate $W$ can be written as the sum of radiative ($W_{rad}$) and nonradiative decay ($W_{nonrad}$):

$$W = W_{rad} + W_{nonrad}. \tag{1}$$

In order to study the luminescence quantum efficiency of the $R$ line luminescence, PL decay measurements were done for samples brought into contact with liquids with different refractive indices. Figure 3 shows decay traces measured at a wavelength of 694.3 nm ($R_1$ line) for an $Al_2O_3$ sample implanted with $3.0\times10^{15}$ Cr/cm$^2$ annealed at 1450 °C for 2 h for the sample in air ($n=1.00$) and the sample in contact with 2-methoxy-4 propenylphenol ($n=1.57$). The experi-

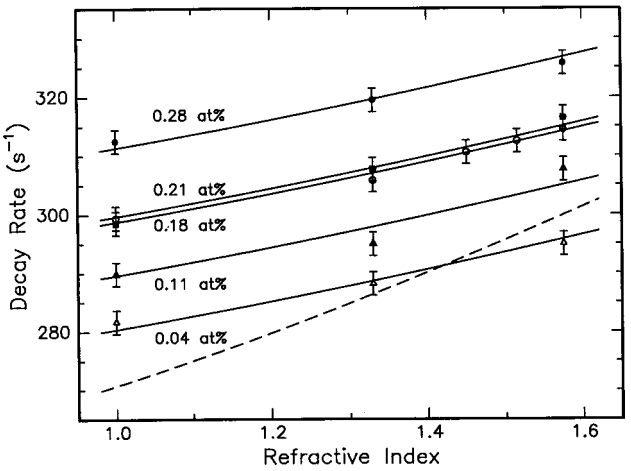


FIG. 4. Measured $R$ line decay rate as a function of the refractive index of the covering liquid. Data are shown for samples with Cr peak concentrations of 0.04, 0.11, 0.18, 0.21, and 0.28 at. % annealed at 1450 °C for 2 h. The dotted line shows the calculated decay rate as a function of the refractive index of the liquid based on the calculated optical DOS, assuming purely radiative decay of 310 $s^{-1}$ for bulk sapphire. The solid line is a fit to all data points assuming a constant radiative decay rate for all samples independent of concentration but a different nonradiative decay rate for each sample.

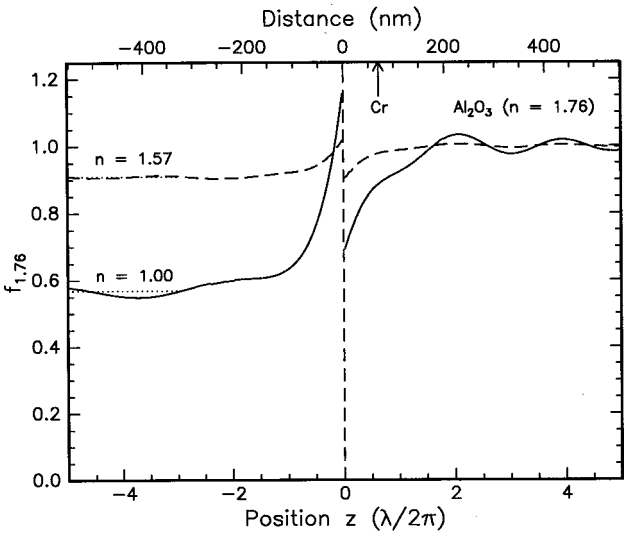


FIG. 5. Polarization- and angle-averaged optical DOS $f_{1.76}$ as a function of position calculated for an $Al_2O_3$ sample in contact with air ($n=1.00$, solid line), and with a liquid with refractive index of 1.57 (dashed line). The optical DOS is normalized to the optical DOS in bulk sapphire ($n=1.76$). The position of the peak of the ion-implanted Cr distribution is indicated by the arrow.

mental configuration is shown in the inset of Fig. 3. A clear increase in the decay rate from 299 to 314 $s^{-1}$ is observed upon adding the liquid.

We have performed similar measurements of the decay rate of the $R_2$ line at a wavelength of 692.9 nm and found no difference in decay rate between the $R_1$ and $R_2$ lines. This agrees with the notion that at room temperature the $R$ lines are expected to be in thermal equilibrium due to the small energy difference of 29 $cm^{-1}$. We have also performed temperature dependent measurements of the PL intensity and PL decay rate (not shown), which indicated that the $R$ lines are in full thermal equilibrium for temperatures above 150 K as observed earlier.[29]

Figure 4 shows measured decay rates for samples in air and brought into contact with liquids with refractive indices of 1.33, 1.45, 1.51, and 1.57, respectively. Decay rates were measured for samples implanted with 0.6, 1.6, 2.5, 3.0, and $4.0\times10^{15}$ $Cr/cm^2$ that were annealed at 1450 °C for 2 h. As can be seen the decay rate increases with refractive index of the liquid and, for a given index, the decay rate increases for increasing Cr concentration.

The increase with index can be explained by calculating the local optical density of states for the Cr ions close to the interface, where the presence of the liquid modifies the optical surrounding of the atom. Local field effects can play a role on length scales between wavelength and atomic scales. In our calculation we have assumed that the presence of the liquid at the interface does not affect the local field around the Cr ion.[30,31] Since the outer $3d$ shell of the Cr ion is involved in the optical transition, the transition frequency is determined by the field at the position of the atom and is extremely sensitive to the local field. In the experiment we did not observe spectral shifts or changes in the line shape, suggesting that the local field is not influenced by the liquids.

Using the dipole approximation, the spontaneous emission rate can be obtained from Fermi's golden rule.[6,12]

$$W_{\mathrm{rad}}(z)=\frac{\pi\omega}{\hbar\epsilon(z)}|D|^2\rho(\omega,z), \tag{2}$$

where $D$ is the dipole matrix element of the $^2E\rightarrow{}^4A_2$ electronic transition at a frequency $\omega$. $\rho$ is the polarization- and angle-averaged local DOS[6,13] at a distance $z$ from the interface, and $\epsilon(z)$ is the position-dependent dielectric constant. The matrix element $D$ depends on the local environment of the emitting Cr ions and is not influenced by the optical properties of the interface or the presence of a liquid. Therefore the only parameter varied in our experiments is the local DOS $\rho(\omega,z)$ at a fixed frequency determined by the $R$ line.

The radiative decay rate $W_{\mathrm{rad}}$ can be expressed more conveniently in terms of an optical DOS $f_{1.76}$, which differs by a factor of $\epsilon$ from the local DOS[32] introduced earlier. This optical DOS is normalized to the DOS for bulk $Al_2O_3$ with a refractive index of 1.76. The total decay rate $W(n,z)$ for a Cr ion at position $z$, with the sample covered by a liquid with index $n$, can now be written as

$$W(n,z)=f_{1.76}(n,z)W_{\mathrm{rad}}^{1.76}+W_{\mathrm{nonrad}}, \tag{3}$$

where $W_{\mathrm{rad}}^{1.76}$ is the radiative decay rate in bulk $Al_2O_3$. The nonradiative decay rate is assumed to be independent of $z$ and $n$.

Figure 5 shows a calculation of the optical DOS $f_{1.76}$ as a function of the distance $z$ from the dielectric interface. The solid line shows the result of a calculation for a system with an infinite half space of $Al_2O_3(n=1.76)$ and an infinite half space of air ($n=1.00$). We have neglected the effect of the Cr ions on the refractive index in our calculations, because for the highest Cr concentration of 0.3 at % the change in refractive due to the Cr is less than 0.01. The interface is positioned at $z=0$. The dashed line shows the calculation for $Al_2O_3$ in contact with a medium with a refractive index of 1.57. In both cases, the optical DOS is discontinuous at the

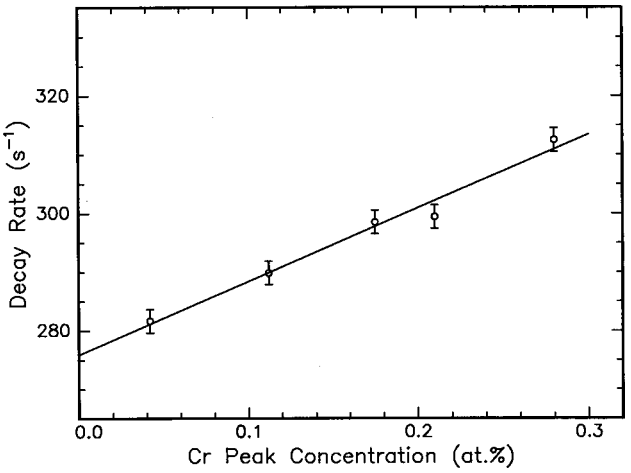


FIG. 6. PL decay rate as a function of Cr peak concentration after annealing at 1450 °C for 2 h. The solid line is a linear fit through the data. The extrapolated PL decay rate for zero Cr concentration is 276 $s^{-1}$.

interface due to a discontinuity of the polarization component parallel to the interface. The oscillations on both sides of the interface are caused by interference between incoming and reflecting waves and have a periodicity of $\sim\lambda/2n$. The position of the peak of the Cr distribution is indicated by the arrow. Figure 5 shows that the radiative decay rate is suppressed towards the interface compared to the bulk value. At the position of the Cr ions the rate increases for increasing refractive index of the liquid. This observation is supported by the data in Figs. 3 and 4.

To calculate the effect of the change in local DOS on the Cr decay rate, we integrated the optical DOS over $z$ using the measured Cr distribution from Fig. 1 for refractive indices in the range of 1.00–1.76. The result of this calculation is shown by the dotted line in Fig. 4, assuming only radiative decay ($W_{\mathrm{nonrad}}=0$) and a radiative decay rate for bulk $Al_2O_3$ of 310 $s^{-1}$. Note that the radiative decay rate is just a scaling factor in the calculation; in this example the value of 310 $s^{-1}$ is arbitrarily chosen such that the calculated relative variation with refractive index can be compared to the data.

By comparing the dashed line in Fig. 4 with the measured data, which show a much weaker increase with $n$, it is clear that the data cannot be described by assuming radiative decay only. The data can be fitted if a nonradiative decay component that is independent of $n$ is introduced as given by Eq. (3). The solid lines show a single fit to all data in Fig. 4 assuming the same bulk radiative rate for all concentrations, but a different nonradiative rate for each sample. This results in $W_{\mathrm{rad}}^{1.76}=164\pm10\,\mathrm{s}^{-1}$ for the radiative decay rate in bulk sapphire. The radiative rate at the position of the implanted Cr ions is $143\pm10\,\mathrm{s}^{-1}$ and is lower than the bulk value due to the reduced local DOS near the interface. The nonradiative rates are $137\pm10$, $146\pm10$, $156\pm10$, $155\pm10$, and $168\pm10\,\mathrm{s}^{-1}$ for the samples implanted with 0.6, 1.6, 2.5, 3.0, and $4.0\times10^{15}\,\mathrm{Cr/cm}^2$, respectively, corresponding to internal quantum efficiencies ranging from 46% to 51% for bulk sapphire.

Figure 6 shows the PL decay rate (measured in air) as a function of Cr peak concentration after annealing at 1450 °C for 2 h. The decay rate increases linearly with Cr concentration which can be explained by assuming an energy migration process between Cr ions that leads to nonradiative decay (''concentration quenching'').[33,34] Extrapolating the PL decay rate to zero Cr concentration, where no energy migration takes place, leads to a decay rate of $276\pm10\,\mathrm{s}^{-1}$. This value is higher than the radiative decay rate of Cr ions near the interface as found above ($143\pm10\,\mathrm{s}^{-1}$). Note that reabsorption of the $R$ line luminescence, which could lengthen the observed decay, can be neglected for our samples due to their thin film geometry in combination with a small absorption coefficient ($\sim10\ \mathrm{cm}^{-1}$), as was observed earlier for Cr-doped $Al_2O_3$ samples of different thickness.[35] We also note that the PL spectra were identical for all Cr concentrations, suggesting that an increased Cr concentration does not change the local field, nor does it lead to significant Cr–Cr pair formation.

A possible explanation for this difference is the existence of a nonradiative decay channel that is associated with defects remaining from the ion implantation, independent of Cr concentration. Alternatively, it could be that for concentrations lower than those studied in Fig. 6 the decay rate does not depend linearly on Cr concentration and would in fact extrapolate to the measured value of $W_{\mathrm{rad}}$. Such an effect was found earlier in Er implanted alkali-borosilicate glasses,[33] in which ion beam induced defects introduced additional nonradiative decay paths of which the density depends on the implanted fluence.

Our experimentally determined radiative decay rate of $164\pm10\,\mathrm{s}^{-1}$ is lower than the value of 250 $s^{-1}$, corresponding to a lifetime of 4 ms, reported in literature.[29,35] This could be due to a difference in the local environment of the Cr in our ion-implanted samples compared to bulk sapphire doped with Cr ions using different methods. This observation is supported by the line broadening observed in Fig. 2, which might be due to residual stress or defects that are not completely annealed out after implantation.

## IV. CONCLUSION

Ion implantation followed by thermal annealing can be used to dope a well-defined near-surface region of sapphire with optically active $Cr^{3+}$ ions. Thermal annealing at 1450 °C is required to remove all implantation damage and leads to the incorporation of at least 95% of the Cr ions on a substitutional position, presumably in the Al sublattice.

Photoluminescence decay rates at a wavelength of 694 nm were measured in air and as a function of refractive index for a range of transparent liquids ($n=1.33$–$1.57$) covering the sample. The decay rate was found to increase with the refractive index of the liquid. From a comparison of the measured decay rates with calculations of the local optical density of states, the radiative decay rate was determined to be $164\pm10\,\mathrm{s}^{-1}$ independent of Cr concentration. A concentration-dependent nonradiative decay rate was found that ranged from $137\pm10\,\mathrm{s}^{-1}$ for 0.04 at. % Cr to $168\pm10\,\mathrm{s}^{-1}$ for 0.28 at. % Cr. These well-characterized samples can now be used to probe the optical DOS in more compli-

cated photonic systems such as strongly absorbing media, scattering media, or photonic crystals.

## ACKNOWLEDGMENTS

The authors gratefully acknowledge discussions with Professor Ad Lagendijk and Dr. Adriaan Tip. This work was part of the scientific program of the Foundation of Fundamental Research on Matter (FOM) and was made possible by financial support from the Dutch Organization for Scientific Research (NWO).

[1] E. M. Purcell, Phys. Rev. **69**, 681 (1946).
[2] W. Lukosz and R. E. Kunz, Opt. Commun. **31**, 42 (1979).
[3] K. H. Drexhage, J. Lumin. **1,2**, 693 (1970).
[4] W. L. Barnes, J. Mod. Opt. **45**, 661 (1998).
[5] R. R. Chance, A. Prock, and R. Silbey, J. Chem. Phys. **62**, 771 (1975).
[6] E. Snoeks, A. Lagendijk, and A. Polman, Phys. Rev. Lett. **74**, 2459 (1994).
[7] E. Yablonovitch, T. J. Gmitter, and R. Bhat, Phys. Rev. Lett. **61**, 2546 (1988).
[8] A. Tip, Phys. Rev. A **56**, 5022 (1997).
[9] H. T. Dung, L. Knöll, and D.-G. Welsch, Phys. Rev. A **57**, 3931 (1998).
[10] H. Khosravi and R. Loudon, Proc. R. Soc. London, Ser. A **433**, 337 (1991).
[11] H. Khosravi and R. Loudon, Proc. R. Soc. London, Ser. A **436**, 373 (1992).
[12] H. P. Urbach and G. L. J. A. Rikken, Phys. Rev. A **57**, 3913 (1997).
[13] B. A. van Tiggelen and E. Kogan, Phys. Rev. A **49**, 708 (1994).
[14] R. M. MacFarlane, J. Chem. Phys. **39**, 3118 (1963).
[15] S. Sugano and M. Peter, Phys. Rev. **122**, 381 (1961).
[16] S. Sugano, Y. Tanabe, and H. Kamikura, *Multiplets of Transition-Metal Ions in Crystals* (Academic, New York, 1970).
[17] T. H. Maiman, Phys. Rev. **123**, 1145 (1961).
[18] T. H. Maiman, R. H. Hoskins, I. J. Haenens, C. K. Asawa, and V. Evthuhov, Phys. Rev. **123**, 1151 (1961).
[19] J. H. Eggert, K. A. Goettel, and I. F. Silvera, Phys. Rev. B **40**, 5724 (1989).
[20] J. H. Eggert, K. A. Goettel, and I. F. Silvera, Phys. Rev. B **40**, 5733 (1989).
[21] Y. Sato-Sorensen, J. Appl. Phys. **60**, 2985 (1986).
[22] W. L. Vos and J. A. Schouten, J. Appl. Phys. **69**, 6744 (1991).
[23] G. C. Farlow, C. W. White, C. J. McHargue, and B. R. Appleton, Mater. Res. Soc. Symp. Proc. **27**, 395 (1984).
[24] H. Naramoto, C. W. White, J. M. Williams, C. J. McHargue, O. W. Holland, M. M. Abraham, and B. R. Appleton, J. Appl. Phys. **54**, 683 (1982).
[25] C. W. White, G. C. Farlow, C. J. McHargue, P. S. Sklad, and B. R. Appleton, Nucl. Instrum. Methods Phys. Res. B **7/8**, 473 (1985).
[26] Ning Yu, Q. Wen, D. R. Clarke, P. C. McIntyre, H. Kung, M. Nastasi, T. W. Simpson, I. V. Mitchell, and D. Q. Li, J. Appl. Phys. **78**, 5412 (1995).
[27] Q. Wen, D. R. Clarke, N. Yu, and M. Nastasi, Appl. Phys. Lett. **66**, 1995 (1995).
[28] D. E. McCumber and M. D. Sturge, J. Appl. Phys. **34**, 1682 (1963).
[29] D. F. Nelson and M. D. Sturge, Phys. Rev. **137**, A1117 (1964).
[30] G. L. J. A. Rikken and Y. A. R. R. Kessener, Phys. Rev. Lett. **74**, 880 (1995).
[31] F. J. P. Schuurmans, D. T. N. de Lang, G. H. Wegdam, R. Sprik, and A. Lagendijk, Phys. Rev. Lett. **80**, 5077 (1999).
[32] R. Sprik, B. A. van Tiggelen, and A. Lagendijk, Europhys. Lett. **35**, 265 (1996).
[33] E. Snoeks, P. G. Kik, and A. Polman, Opt. Mater. **35**, 265 (1996).
[34] H. C. Chow and R. C. Powell, Phys. Rev. B **21**, 3785 (1980).
[35] N. A. Tolstoi and L. Shun'-Fu, Opt. Spectrosc. **13**, 224 (1962).